Comparison of actual evapotranspiration by the google earth engine evapotranspiration flux (EEFlux) to the METRIC model using remote sensing data and in-situ climate observations

Omar Alsanjar[1*], *Mahmut* Cetin[1]

[1]Cukurova University, Department of Agricultural Structures and Irrigation, Adana, Turkiye

Abstract. Actual evapotranspiration (ETa) is essential data in developing water budgets and calculating irrigation water requirements in large-scale irrigation schemes. Nowadays, remote sensing (RS)-based surface energy balance models help us estimate ETa with high resolution when compared to direct methods that focus only on a single point in a field. This study aimed both at estimating ETa by Mapping EvapoTranspiration at high Resolution with Internal Calibration (METRIC) and Google Earth Engine Evapotranspiration Flux (EEFlux) platform and comparing reference evapotranspiration based on the Penman-Monteith equation (ETo) with ETa by the METRIC and EEFlux in a sub-catchment (A=9495 ha) under irrigation, located in the Lower Seyhan Plain (LSP), Turkiye in the 2020 hydrological year. For this purpose, 16 Landsat 7 and Landsat 8 images, local climatic data acquired from two meteorological stations in the catchment, and CFSv2 gridded global data were used. Results showed a good agreement between ETa-EEFlux with ETa-METRIC. Moreover, a strong correlation was found between ETo and ETa-METRIC (r=0.93 and slope close to 1 and RMSE value of 0.74 mm day^{-1}) if compared to the relationship between ETo with ETa-EEFlux. The results show the potential of applying the METRIC model and EEFlux for mapping ETa over a large-scale irrigation scheme.

1 Introduction

Actual Evapotranspiration (ETa) is a crucial input for the water cycle, developing water budgets and calculating net irrigation water requirements, agricultural water management, and hydrological modelling, among others. The typical character of all direct methods is to compute ETa at a point scale such as the soil water budget approach, lysimeters, eddy covariance, and scintillometer. Therefore, these techniques generally fail to show the ETa variations in the field [1] if compared to the remote sensing (RS)-based surface energy balance models [2-4]. Among RS-based surface energy balance models is the Mapping Evapotranspiration at high Resolution with Internalized Calibration (METRIC) model [5-6], which is one of the more widely used to estimate ETa in operational irrigation practices at a large scale. As known commonly, the METRIC model applies principles and techniques that originated with the Surface Energy Balance Algorithms for Land (SEBAL) [7].

The METRIC model has been applied to estimate ETa in different regions of the world using satellite images with ground truth data. The accuracy of ETa by the METRIC model was compared to ETa measured by the lysimeter, the Bowen ratio, and eddy covariance towers for several crops in a range of locations of the world with errors ranging from 3–20% [5, 8, 9]. These results proved a good agreement between ETa by the METRIC model and ETa by the direct method. However, the applying METRIC model requires well-trained experts who have good experience dealing with RS data and selecting the anchor pixels, i.e., hot and cold pixels. Furthermore, this model study consumes time to estimate ETa for one image [10]. For this reason, automated calibration algorithms for the METRIC model were designed to reduce the errors that might happen to the users. For example, the R-METRIC was applied based on the METRIC model over a large irrigation catchment, i.e., Akarsu Irrigation District (AID) in Turkiye [2, 4], which automatized hot and cold pixel selection that decreased the possibility of human error [11].

The fact is that automated calibration algorithms for the METRIC model require several data such as satellite images, cloud mask, digital elevation model (DEM), local climate data, soil type map, and land cover map/land use or

*Corresponding-author:omarsenjar@yahoo.com

cropping patterns, among others. These data need to make some pre-processing before applying the METRIC model, and thus consume time for the users. For this reason, the Earth Engine Evapotranspiration Flux (EEFlux) application has been designed and developed on the Google Earth Engine (GEE) platform based on the METRIC model [6] to save time and money. Moreover, this platform can quickly produce ETa at 30 m spatial resolution with other products such as surface temperature (Ts), normalized difference vegetation index (NDVI), DEM, and albedo.

ETa estimation by the EEFlux and METRIC model at a 30 m resolution scale can be useful for hydrological applications as well as agricultural water management and water balance calculations at large-scale irrigation catchments. However, as reported by many researchers [2, 4, 5, 7], research results need some sort of justification and/or validation. The novelty of this study is to compare the ETa by the EEFlux product with the ETa-METRIC model for checking the accuracy of the EEFlux product over AID during the 2020 water year. Therefore, the aim of this paper is to a) compare the ETa values from EEFlux with the METRIC model to assess the utility and accuracy of EEFlux products, and b) find the relationship between ETa by the METRIC model and EEFlux with reference evapotranspiration, i.e., ETo, by FAO-Penman-Monteith approach. Furthermore, this methodology can be generalized for checking ETa which is produced by EEFlux to the METRIC model and ETo in a range of climate locations and zones of the world.

2 Material and method

2.1 Study area and meteorological data

The study area, Akarsu Irrigation District (hereafter, AID, A=9495 ha) is situated in the Lower Seyhan Plain (LSP) as part of the southeastern Mediterranean region of Turkiye (Fig. 1).

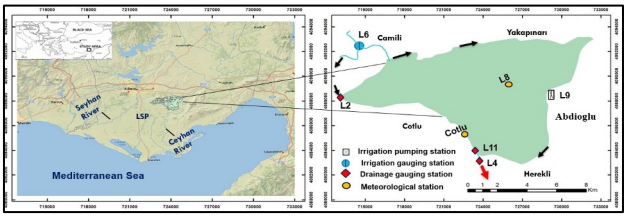

Fig. 1. The study area is located in the southeastern Mediterranean region of Turkiye. Meteorological stations are L8 and Cotlu located in the study area. L6 and L9 stand for irrigation water input locations; L2 and L11 stand for drainage water input locations, and L4 drainage output at the outlet of the catchment.

The AID has been irrigated for more than 60 years and is located between 36° 57′ 32″ and 36° 50′ 43″ N latitudes and 35° 40′ 22″ and 35° 28′ 42″ E longitudes. The study area is characterized by warm and rainy in the winter season while dry and hot in the summer season due to the Mediterranean climate type dominating in the LSP. The annual daily average, minimum, and maximum air temperatures are 18.9°C, 9.0ºC, and 31.0ºC, respectively [4]. The mean annual precipitation of the basin is around 650 mm [12]. Local climatic data acquired from L8 and Cotlu meteorological stations -installed in the study area- were used for the METRIC model while EEFlux used CFSV2 gridded weather data globally. In turn, hourly and daily climate data (temperature, wind speed, solar radiation, relative humidity, and precipitation) were subjected to quality control (QC) checks such as gaps in the data, outliers, constant values, jumps, etc., before using them to cover the 2020 water year. Water year in Turkiye has been defined as the period, with a length of 365 days, between October 1st of one year and September 30th of the next.

2.2 Remotely sensed data

To perform the METRIC model by using local meteorological data acquired in the study area, in total 16 clear-sky Landsat satellite images were downloaded from the USGS website (http://earthexplorer.usgs.gov) (path 175, row 34) and used in this research. On the other hand, EEFlux is based on the Google Earth engine, which can use 16 Landsat images in the cloud through (METRIC-EEFlux (eeflux-level1.appspot.com)). The type of Landsat images used in this research is Landsat 7 and Landsat 8 with 30 m by 30 m spatial resolution. General characteristics of the Landsat satellite images are given in Table 1. The cloud mask was applied by the Environment for Visualizing Images (ENVI) software program for two satellite images in January and February 2020, i.e., DOY 28 and DOY 60 as seen in Table 1.

Table 1. Availability of Landsat 7, and Landsat 8 scene information in the 2020 water year: names of scenes, acquisition dates, and overpass local time.

Image	Day of the year (DOY)	Landsat scene	Satellite	Cloud cover (%)	Acquisition dates	Overpass local time (AM)
1	273	LC81750342019273LGN00	Landsat 8	0	30.09.2019	11:16:02.5052379
2	297	LE71750342019297SG100	Landsat 7	16	24.10.2019	10:59:54.3561211
3	321	LC81750342019321LGN00	Landsat 8	4	17.11.2019	11:16:01.7353690
4	353	LC81750342019353LGN01	Landsat 8	1	19.12.2019	11:15:58.3225900
5	28	LE71750342020028NPA00	Landsat 7	67	28.01.2020	10:55:13.3874493
6	60	LE71750342020060SG100	Landsat 7	66	29.02.2020	10:53:33.8472536
7	68	LC81750342020068LGN00	Landsat 8	2	8.03.2020	11:15:36.2460760
8	108	LE71750342020108SG100	Landsat 7	6	17.04.2020	10:50:52.5176873
9	148	LC81750342020148LGN00	Landsat 8	4	27.05.2020	11:15:08.7684079
10	180	LC81750342020180LGN00	Landsat 8	1	28.06.2020	11:15:26.9694210
11	196	LC81750342020196LGN00	Landsat 8	1	14.07.2020	11:15:33.4238989
12	212	LC81750342020212LGN00	Landsat 8	0	30.07.2020	11:15:37.9038700
13	228	LC81750342020228LGN00	Landsat 8	0	15.08.2020	11:15:42.0945460
14	244	LC81750342020244LGN00	Landsat 8	0	31.08.2020	11:15:50.3682170
15	260	LC81750342020260LGN00	Landsat 8	1	16.09.2020	11:15:56.5028510
16	300	LE71750342020300SG100	Landsat 7	8	26.10.2020	10:38:56.1154274

2.3 EEFLUX and METRIC model

EEFlux-METRIC product and METRIC model were applied to estimate actual evapotranspiration (ETa, hereafter, ETa-EEFlux and ETa-METRIC) for each pixel and the whole study area (Eq. 1) using Landsat satellite imagery and climatic variables acquired by hourly CFSv2 operational analysis [13] and ground-based hourly weather data from L8 and Cotlu weather stations in the study area at the time of satellite overpass, primarily based on [5-6].

$$LE = R_n - G - H \quad (1)$$

Where *LE* stands for latent heat, *Rn* is net radiation, *H* is sensible heat, and *G* is soil heat flux. All the fluxes are in the unit of watt per meter square (i.e., W m^{-2}). EEFlux was performed by the Google Earth engine, while the standard METRIC model was through the R-METRIC model using a water package in the R program [11] and LandMOD ET mapper-MATLAB [14-15]. Reference evapotranspiration (ETo) in mm day^{-1} unit was applied by the FAO-Penman-Monteith approach [15-16]. Further information on the EEFlux-METRIC and METRIC model and equations, i.e., ETa calculation, are given by [6, 10, 15].

In this study, the difference between ETa-METRIC and ETa-EEFlux was statistically assessed by using a simple linear regression approach over the AID at the satellite image acquisition dates. Furthermore, root mean square error (RMSE) and coefficient of determination (R^2) were applied in this research for statistical inference.

3 Results and discussion

3.1 EEFlux vs. METRIC comparisons

In this paper, EEFlux was applied to estimate ETa using CFSV2 gridded weather data over the study area. On the other hand, in the METRIC model, ETa was estimated by employing the R-METRIC and LandMOD ET mapper-MATLAB to drive spatiotemporal ETa data using local ground truth data at satellite image acquisition dates over the AID. For example, Fig. 2 shows the daily ETa and land surface energy balance (SEB, i.e., LE, Rn, H, and G) components as an example on 15.08.2020 which coincides with the day of the year (DOY) 228. Finally, the ETa values by the EEFlux and METRIC model were compared with ETo values at the satellite image acquisition dates.

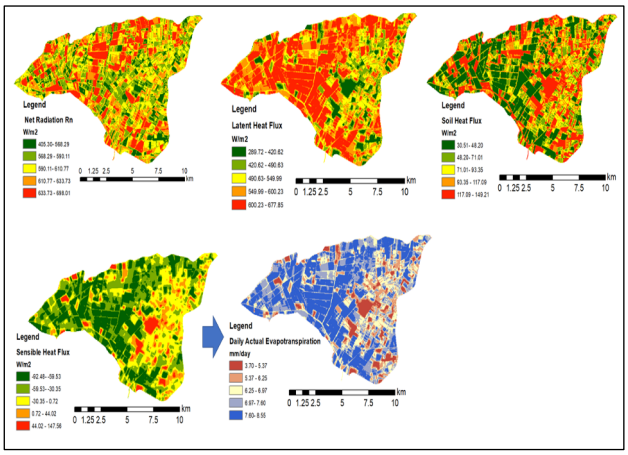

Fig. 2. Spatial distribution of ETa and SEB fluxes over the irrigated catchment on DOY 228 (August 15, 2020): Net radiation (Rn, top left), latent heat flux (LE, top mid), sensible heat flux (H, top right), soil heat flux (G, bottom left), and Actual evapotranspiration (ETa, bottom mid) in the unit of mm day^{-1} for ETa and W m^{-2} for all SEB.

The variation of ETa-METRIC, ETa-EEFlux, and ETo by the FAO-Penman-Monteith method [16] in the study area was presented in Fig. 3 at the time of the satellite overpass. As seen in Fig. 3, the ETo values were slightly higher than ETa-METRIC and ETa-EEFlux together, except on DOY 353, DOY 28, DOY 228, and DOY 244. These results can be interpreted by the Kc, i.e., the ETrFi value in the METRIC model, which is greater than 1.0. This fraction in the METRIC model considers all factors of climate, soil, and plant types together. Therefore, this fraction is a more representative value as compared to the standard Kc values documented by Allen et al. [16].

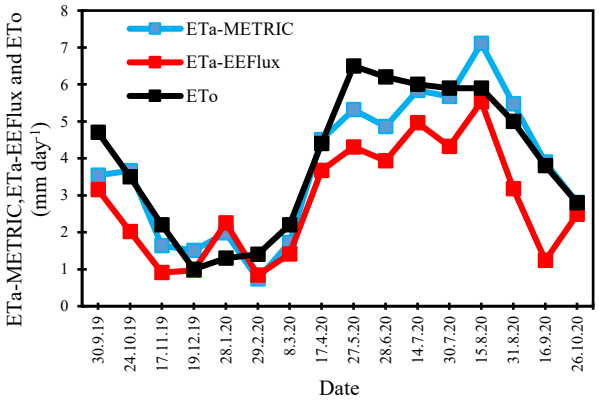

Fig. 3. Temporal variations of areal mean daily ETa values, acquired by the EEFlux and METRIC approach with ETo, at the time of satellite overpass over the AID.

3.2 Linear regression analysis

In this study, linear regression analysis has been applied to assess the relationship between ETa-METRIC and ETa-EEFlUX over the study area (Table 2). The comparison between ETa-METRIC and ETa-EEFlux was drawn through a scatter diagram over the study area (Fig. 4).

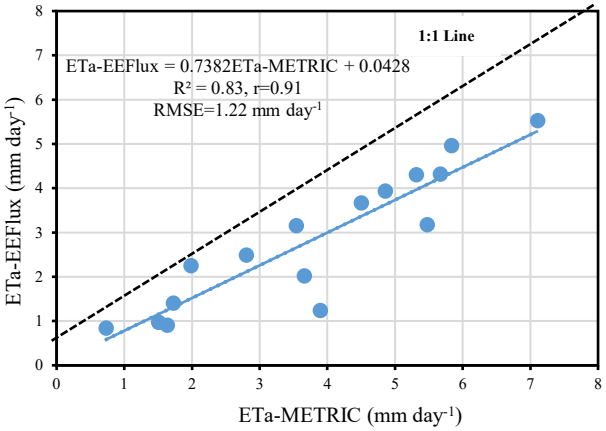

Fig. 4. Comparison between ETa-EEFlux and METRIC models for agricultural fields located in AID in the 2020 water year.

Similarly, we applied the same method to find the linear relationship between ETo and ETo-EEFlux, ETo with ETa-METRIC and ETa-EEFlux, and calculate RMSE for each linear model as shown in Table 2. As seen in Table 2, the agreement found between ETa by METRIC and EEFlux, and ETo by the FAO-Penman-Monteith with ETa through METRIC model and EEFlux are considered a good indicator of strong correlation and similarity in algorithm performance between EEFlux and METRIC. A strong correlation was found between ETo and ETa by the METRIC with R^2 and slope close to 1 and RMSE value of 0.74 if compared to the relationship between ETo with ETa-EEFlux (Table 2).

Table 2. Performance statistics of ETa by the METRIC model, EEFlux, and ETo by the FAO-Penman–Montieth over the study area.

	Linear Model	**RMSE (mm day^{-1})**	**R^2**	**r**
ETa-METRIC and ETa-EEFlux	ETa-EEFlux= 0.7382* ETa-METRIC + 0.0428	1.22	0.83	0.91
ETo and ETo-EEFlux	ETo-EEFlux = 0.979* ETo + 0.3583	0.73	0. 88	0.93
ETo and ETa-EEFlux	ETa-EEFlux = 0.7023*ETo + 0.0679	1.42	0.77	0.88
ETo and ETa-METRIC	ETa-METRIC = 0.9142*ETo + 0.1798	0.74	0.86	0.93

4 Conclusion

This research presents the first attempt to compare the ETa by the EEFlux and the METRIC model with ETo in the study area using RS data (Landsat 7 and Landsat 8) coupled with local and global climatic variables during the 2020 water year. EEFlux results show a good agreement with METRIC for the entire study area. In addition, a strong correlation was found between ETo with ETa by the METRIC model as compared to the relationship between ETo with ETa-EEFlux. It can be concluded that ETa maps generated by the METRIC model and EEFlux can be used in hydrological modelling practices, the development of water budgets, and agricultural water management at the catchment level.

Acknowledgements

The authors thank the Scientific Research Projects (BAP) Coordination Unit of Cukurova University [Project Number: FDK-2022-14907].

Funding

This work was supported by the Scientific Research Projects (BAP) Coordination Unit of Cukurova University [Project Number: FDK-2022-14907].

References

1. X.C Zhang, J.W Wu, H.Y Wu, Y Li. WaterSci Eng., **4**, 24–35 (2011)
2. M. Cetin, O. Alsenjar, H. Aksu, M.S Golpinar, M.A Akgul. Hydrological Sciences Journal, (2023a)
3. M. Cetin, O. Alsenjar, H . Aksu, M.S Golpinar, M.A Akgul. Water Supply 00:1 (2023b)
4. O. Alsenjar, M. Cetin, H. Aksu, M.S Golpinar, M.A Akgul. Mediterranean Geoscience Reviews, **5**, 35–49 (2023b)
5. R.G. Allen, M. Tasumi, A. Morse, R. Trezza, J.L. Wright, W.G.M. Bastiaanssen, W. Kramber, L. Lorite, C.W. Robison. J. Irrig. Drain. Eng., **133**, 395–406 (2007a)
6. R.G. Allen, M. Tasumi, R Trezza. J. Irrig. Drain. Eng., **133**, 380–394 (2007b)
7. W.G.M. Bastiaanssen, M. Menenti, R.A. Feddes, A.A.M. Holtslag. J. Hydrol., 212–213:198–212 (1998a)
8. M. Mkhwanazi, J.L. Chávez HydrologyDays2013.http://www.hydrologydays.colostate.edu/Papers_13/Mkhwanazi_paper pdf (2012)
9. R. Madugundu, K.A. Al-gaadi, E. Tola, A.A. Hassaballa, V.C. Patil. Hydrol. Earth Syst. Sci., **21** 6135-6151 (2017)
10. F. Foolad, P. Blankenau, A. Kilic, R.G. Allen, J.L. Huntington, T.A. Erickson, D. Ozturk, C.G. Morton, S. Ortega, I. Ratcliffe, T.E. Franz, D. Thau, R. oore, N. Gorelick, B. Kamble, P. Revelle, R. Trezza, W. Zhao, C.W. Robison. Preprints, 2018070040 https://doi.org/10.20944/preprints201807.0040.v1 (2018)
11. G.F. Olmedo, S. Ortega-farias, D. Fonseca-luengo. The R Journal Vol. XX/YY, AAAA 20ZZ, ISSN 2073-4859 doi:10.32614/RJ-2016-051 (2016)
12. M. Cetin, H. Kaman, C. Kirda, S. Sesveren. Fresenius Environmental Bulletin (FEB), **29**(05), 3409-3414 (2020)
13. X. Yuan, E.F. Wood, L. Luo, M.A. Pan. Geophys. Res. Lett., **38**, 712 doi: 10.1029/2011GL047792 (2011)
14. N. Bhattarai, L.J. Quackenbush, J. Im, S.B. Shaw Remote Sensing of Environment, **196**, 178-192 (2017)
15. O. Alsenjar, M. Cetin, H. Aksu, M.A. Akgul, M.S. Golpinar. Journal of Agricultural Sciences 29(2):677-689 doi:10.15832/ankutbd.1174645 (2023a)
16. R.G. Allen, L.S. Pereira, D. Raes, M. Smith. FAO Irrigation and Drainage, pp. 56 FAO, Rome (1998)